NJC

Accepted Manuscript

This is an *Accepted Manuscript*, which has been through the Royal Society of Chemistry peer review process and has been accepted for publication.

Accepted Manuscripts are published online shortly after acceptance, before technical editing, formatting and proof reading. Using this free service, authors can make their results available to the community, in citable form, before we publish the edited article. We will replace this *Accepted Manuscript* with the edited and formatted *Advance Article* as soon as it is available.

You can find more information about *Accepted Manuscripts* in the Information for Authors.

Please note that technical editing may introduce minor changes to the text and/or graphics, which may alter content. The journal's standard Terms & Conditions and the Ethical guidelines still apply. In no event shall the Royal Society of Chemistry be held responsible for any errors or omissions in this *Accepted Manuscript* or any consequences arising from the use of any information it contains.

ROYAL SOCIETY OF CHEMISTRY

www.rsc.org/njc

Cite this: DOI: 10.1039/c0xx00000x

www.rsc.org/xxxxxx

ARTICLE TYPE

DNA-based nanocomposite as electrochemical chiral sensing platform for the enantioselective interaction with quinine and quinidine

Qing Zhang, Yihan Huang, Liju Guo, Cui Chen, Dongmei Guo,Ya Chen, Yingzi Fu*

Received (in XXX, XXX) Xth XXXXXXXXX 20XX, Accepted Xth XXXXXXXXX 20XX
DOI: 10.1039/b000000x

A novel chiral sensing platform, employing biomolecule-based nanocomposite prepared by calf thymus double stranded DNA, methylene blue and multiwall carbon nanotubes (DNA-MB-MWNTs), had been utilized for the discrimination of quinine (QN) and quinidine (QD). The DNA-based nanocomposite, which could be used as electrochemical sensing unit and chiral probe, was characterized by transmission electron microscopy (TEM), ultraviolet-visible spectroscopy (UV-Vis) and cyclic voltammetry (CV). After the proposed sensing platform had interacted with QN and QD, a larger electrochemical signal was obtained from QD. The comparative experiment indicated that the proposed strategy had not only simplified the fabrication processes but also enhanced the enantioselective interaction in chiral analysis. In addition, the experimental factors such as the acidity, the interaction time and the concentration of enantiomers were investigated on the effect of enantioselective interaction.

1. Introduction

Biomolecules in living organism such as DNA and protein are constituted by only one of the enantiomers, right handed or left handed. As a consequence, racemic drugs may perform different physiological effects on pharmacological activity, metabolism process and toxicity in body.[1] With the aim of exploring pharmaceutic benefit and therapeutic application in biological processes, numerous technologies including high performance liquid chromatography,[2] capillary electrophoresis,[3] mass spectroscopy,[4] fluorescence,[5] quartz crystal microbalance [6] and electrochemistry [7] have been employed to monitor the interaction between biomolecules and chiral drugs. Among those, the integration of electrochemical detection with chiral analysis exhibits significant merits such as simple operation, high sensitivity and low cost.[8]

The application of nanomaterial-based strategies in electrochemical analysis has aroused considerable attention because of its fascinating properties such as high surface area, rich electronic conductivity, excellent chemical stability and extremely biocompatibility.[9] Noticeable progress has been made in the utilization of the functionated carbon nanotubes in recent years, in which carbon nanotubes has interacted with organic dyes,[10] biomolecules,[11] polymers,[12] metal or semiconductor nanoparticles [13,14] to develop the ideal miniaturized sensor. It was reported that methylene blue (MB), a phenothiazine electroactive dye, could be adsorbed strongly onto the multiwalled carbon nanotubes (MWNTs) through π - π electronic interaction to form methylene blue - multiwalled carbon nanotubes nanohybrid (MB-MWNT), which could perform excellent redox activities on the surface of electrodes.[15] In addition, MWNTs has been used to windingly disperse with DNA through non-covalent electrostatic effect to form a sensing material for biological applications.[16]

DNA is one of the classes of natural polymers, which consists of a ribose sugar, a phosphate and a heterocyclic aromatic base. Owing to the right handed helical conformation, it has been used as a promising chiral selector to promote the understanding of the selectivity for chiral compounds in biosystem. [17-19] Belonging to the family of cinchona alkaloids, quinine (QN) and quinidine (QD) are stereoisomers, which consist of a planar quinoline and a rigid quinidine ring connected with a secondary methyl alcohol bridge (as shown in Fig.1). They have widely used as highly effective catalysts in asymmetric syntheses, as resolving agents for chiral acids or as chiral selectors in direct enantioseparations.[20,21] At present, chiral analysis of QN and QD has gained increasing attention, and lots of valuable information have been obtained from the previous literatures. For example, as antimalarial drugs, the antimalarial activity of QD is four times bigger than that of QN.[22] QD can inhibit the CYP2D6 isoenzymes for metabolizer phenotypes, while QN has no effect.[23] However, the analogue CYP2D1 isoenzyme in rat is inhibited by QN and not by QD.[24] The interaction between DNA and chiral drugs have utmost importance in pharmacological analysis, gene mutation and disease origins. It was reported that antimalarial compounds could display weak affinity with DNA to inhibit growth of human breast cancer cells,[25] but there is few reports on discussion the stereoselective interaction of DNA with QN and QD.

Herein, in this article, a novel functionated nanomaterial, coupling of the natural chiral selector (DNA), redox-probe indicator (MB) and carbon material (MWNTs), have been prepared to develop a simple strategy in electrochemical chiral analysis of QN and QD. This study may provide a reference to understand the interaction between biomolecule and chiral drugs, and promote the development of electrochemical chiral sensor.

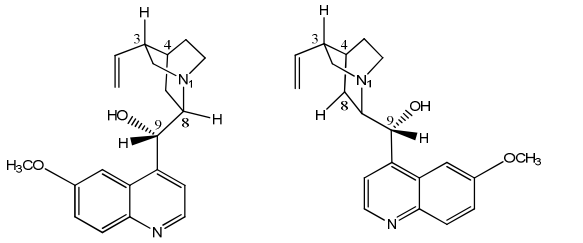

(-)-Quinine (1S, 3R, 4S, 8S, 9R) (+)-Quinidine (1S, 3R, 4S, 8R, 9S)

Fig. 1 Structure of quinine (QN) and quinidine (QD).

2. Experimental

2.1 Materials and Apparatus

Calf thymus double-stranded DNA (DNA), pristine multiwall carbon nanotubes (MWNTs, diameter 15 ± 5 nm, length 1 - 5 μm, purity 95%) and methylene blue (MB, 95%) were purchased from sigma chemical Co. (St. Louis, MO, USA). Quinine (QN, 98%) and quinidine (QD, 98%) were obtained from Aladdin Chemistry Co. (Shanghai, China). 0.1 M phosphate buffer solution (PBS) with various pH were prepared with 0.1 M Na_2HPO_4 and 0.1 M KH_2PO_4 containing 0.1 M KCl. Other chemicals were analytical grade. Double-distilled water was used throughout the study and all experiments were performed at ambient temperature.

Cyclic voltammetry (CV) was performed with a CHI 604D electrochemistry workstation (Shanghai Chenhua Instruments Co., China). Transmission electron microscopy (TEM) was used to estimate the microstructures of the prepared nanocomposite (H600, Hitachi, Japan). Ultraviolet-visible spectroscopy (UV-Vis) was recorded by the UV-2450 spectrometer (Shimadzu, Japan). Fourier transform infrared (FTIR) spectroscopic measurements was performed on a Nicolet 5700 Fourier transform spectrometer (USA). The value of pH was measured by pH meter (MP 230, Mettler-Toledo, Switzerland).

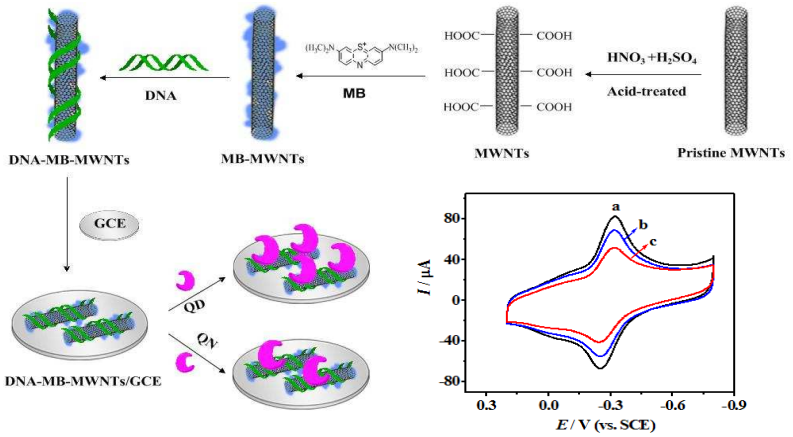

Scheme 1 Preparation procedure of the sensing platform and the cyclic voltammograms of the proposed platform in 0.1 M PBS (pH 7.0) before and after interacted with 1.0 mM QN and QD for 10 min: (a) DNA-MB-MWNTs/GCE; (b) DNA-MB-MWNTs/GCE + QN and (c) DNA-MB-MWNTs/GCE + QD. Scan rate, 100 mV s^{-1}; scan range, -0.8 to 0.2 V (vs. SCE).

2.2 Synthesis of DNA-based nanocomposite

DNA-based nanocomposite was prepared by the following steps: firstly, pristine MWNTs were treated with the mixed HNO_3 and H_2SO_4 (1:3 volume ratio of 68% HNO_3 and 98% H_2SO_4) to introduce carboxyl groups on their surface.[26] After being washed to neutral pH and dried, the acid-treated MWNTs were characterized the existence of carboxyl groups by FT-IR spectra, and the amount of carboxyl groups were determined by acid-base titration technique (Supplementary Information for details). Secondly, the treated MWNTs (1.0 mg) and MB (1.5 mg) were dissolved in double-distilled water (10 mL), following by ultrasonicating for 2 h. The negative charged carboxylic groups of the MWNTs were beneficial to the adsorption of the positive charged MB molecules on the surface of MWNTs through electrostatic interaction. The black product (MB-MWNTs) was collected after centrifuged in 15000 rpm, rinsed with double-distilled water to remove non-integrated MB and dried at 50°C, respectively. Thirdly, the obtained MB-MWNTs (1.0 mg) were ultrasonically dispersed in DNA solution (4 mL, 0.33 mg L^{-1}). After three centrifuge/wash cycles (15000 rpm, 4 °C for 20 min), the black mixed solution of DNA-MB-MWNTs nanocomposite was prepared in double-distilled water (0.5 mg mL^{-1}). The schematic processes of DNA-MB-MWNTs nanocomposite were illustrated in Scheme 1.

2.3 Fabrication of the sensing platform

To obtain mirror-like surface, bare glassy carbon electrode (GCE, Φ = 4.0 mm) was polished sequentially with 1.0, 0.3 and 0.05 μm alumina slurry, and then ultrasonically cleaned in ethanol and double-distilled water about 5 min, respectively. After that, the DNA-MB-MWNTs solution (8.0 μL) was dropped

on the clean GCE surface (denoted as DNA-MB-MWNTs/GCE). MB-MWNTs/GCE were also fabricated for the electrochemical detection. Moreover, DNA solution (8.0 μL, 0.33 mg mL^{-1}) was dropped on MB-MWNTs/GCE to obtain DNA/MB-MWNTs/GCE for comparative research. Prior to be used, modified electrodes were stored in a refrigerator (4°C).

2.4 Experimental measurements

Electrochemical experiments were carried out with three electrode system, in which either the bare or the modified electrode was used as working electrode, a saturated calomel electrode was worked as the reference electrode and a platinum wire was acted as an auxiliary electrode. The peak current of DNA-MB-MWNTs/GCE was regard as I and the peak current after DNA-MB-MWNTs/GCE immersed in QN or QD was regard as I_{QN} or I_{QD}. The difference of the peak current was given by the following equation: $\Delta I_{QN} = I - I_{QN}$, $\Delta I_{QD} = I - I_{QD}$ and $\Delta I = \Delta I_{QD} - \Delta I_{QN}$.

3. Results and discussion

3.1 Characteristics of the DNA-based nanocomposite

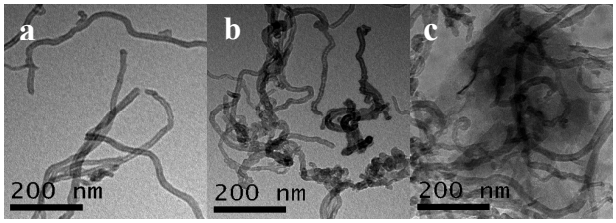

Fig.2 TEM images: (a) MWNTs, (b) MB-MWNTs and (c) DNA-MB-MWNTs.

Transmission electron microscopy (TEM) was employed to characterize the microstructure of nanocomposite (Fig.2). Compared with the randomly cross linked MWNTs (Fig.2a), MB-MWNTs (Fig.2b) appeared numerous spicule-shaped due to the electrostatic interaction between MB and acid-treated MWNTs. Moreover, DNA-MB-MWNTs nanocomposite showed cloudiness and dimness (Fig.2c), indicating that MB-MWNTs were wrapped by the negatively charged DNA.

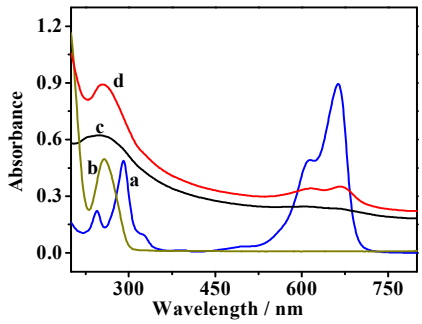

Fig.3 UV-Vis spectra of (a) MB, (b) DNA, (c) MWNTs and (d) DNA-MB-MWNTs. The concentrations were 0.05, 0.05, 0.05, 0.05 mg mL^{-1}, respectively.

Fig.3 displayed the ultraviolet-visible absorption (UV-Vis) spectra of MB, DNA, MWNTs and DNA-MB-MWNTs solutions. The pure MB had two strong absorption peaks at 291 nm and 663 nm (Fig.3a), the characteristic absorption peak of DNA was at 245 nm (Fig.3b), and the MWNTs showed an absorption peak at 249 nm (Fig.3c). But the red shift and wider absorption peak were gained for DNA-MB-MWNTs (Fig.3d), suggesting the successful attachment of MB and DNA to MWNTs.

3.2 Electrochemical characteristic of the sensing platform

Fig.4 displayed the cyclic voltammograms (CVs) of different modified electrodes. There were no evident peak signals on bare GCE (Fig.4a) and MWNTs/GCE (Fig.4b) due to the absence of redox probe. While well-defined redox peaks appeared on MB-MWNTs/GCE (Fig.4c), DNA/MB-MWNTs/GCE (Fig.4d) and DNA-MB-MWNTs/GCE (Fig.4e), resulting from the excellent electrochemical activities of MB (redox indicator molecule).[27] The peak current of MB-MWNTs/GCE was about 160.9 μA (Fig.4c). With the successive immobilization of DNA on MB-MWNTs/GCE, the response of DNA/MB-MWNTs/GCE was obtained on 126.4 μA (Fig.4d), due to the fact that biological molecule (DNA) made a blockage of electronic transmission toward the electrode surface. After DNA had interacted effectively with MB-MWNTs to form the proposed nanocomposite (DNA-MB-MWNTs), the peak current about 82.64 μA was observed on DNA-MB-MWNTs/GCE (Fig.4e), indicating the rich existence of DNA containing in the proposed nanocomposite. Moreover, the peak-to-peak separation of DNA-MB-MWNTs/GCE was 75.90 mV and the ratio of cathodic to anodic peak currents was about one, suggesting a quasi-reversible process.[28] Compared with the traditional technology (step by step modification), the proposed nanocomposite has obviously simplified the fabrication processes.

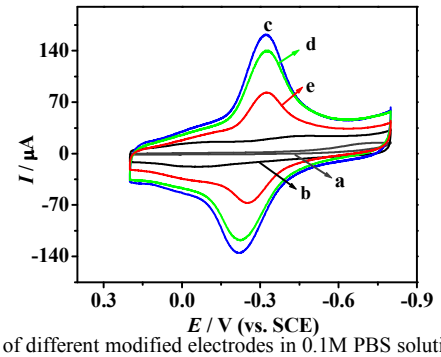

Fig.4 CVs of different modified electrodes in 0.1M PBS solution (pH 7.0): (a) bare GCE, (b) MWNTs/GCE, (c) MB-MWNTs/GCE, (d) DNA/MB-MWNTs/GCE and (e) DNA-MB-MWNTs/GCE. Other conditions, as in Scheme 1

CVs of the DNA-MB-MWNTs/GCE at different scan rates were studied (Fig.5). The peak current increased linearly with the rising scan rate in the range of 50 - 800 mV s^{-1}, as shown in the inset of Fig.5, indicating a surface controlled process. The linear regression equation was $I_0 = 0.2002\ v + 0.2283$ ($R = 0.9964$). It confirmed that MB containing in DNA-MB-MWNTs nanocomposite exhibited excellent electrochemical electron transfer. In addition, the average surface coverage (Γ) of DNA-MB-MWNTs on the electrode surface was calculated to be 1.42×10^{-9} mol cm^{-2}. [29]

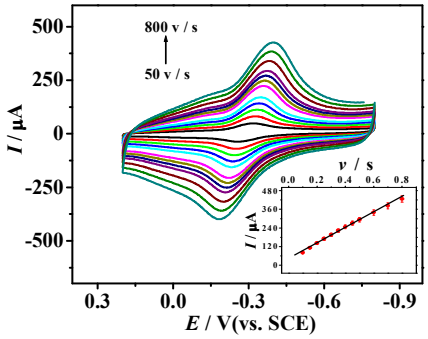

Fig.5 CVs of DNA-MB-MWNTs/GCE at different scan rates.The inset shows the dependence of redox currents on the scan rates. The detection were carried out in 0.1 M PBS (pH 7.0).

Fig.6 exhibited the effect of pH on the CVs of DNA-MB-MWNTs/GCE. It was observed that the rising pH led to a negative shift of the cathodic and anodic peaks. The formal potentials (*E*) had a linear relationship with pH values (curve a in the inset of Fig.6), in which the linear regression equation was calculated as E (V) = -0.0563 pH + 0.5270 (R = 0.9950). The slope of −56.3 mV/pH was close to the theoretical value of −59.0 mV/pH for the $2e^-/2H^+$ redox process,[30] suggesting that the obtained nanocomposite could exhibit excellent electrochemical properties. Additionally, the relationship of peak current with pH was displayed (curve b in the inset of Fig.6), in which the maximum peak was achieved in pH 7.0. This could arise from the hydrogen ion in the solution influenced the redox processes of MB containing in the proposed nanocomposite.[31] Thus, the pH value of 7.0 in the PBS solution was selected for the following investigation.

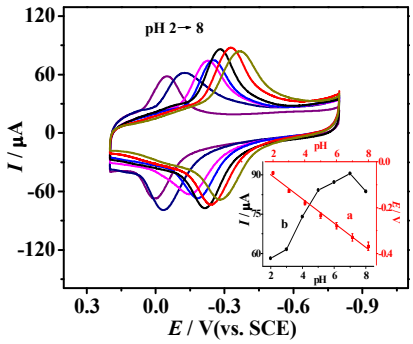

Fig.6 CVs of proposed electrodes in 0.1 M PBS with various pH at 100 mV s^{-1}. Inset showed the effect of pH on (a) formal potential and (b) peak current.

3.3 The interaction between the sensing platform and QN or QD

As illustrated in Scheme 1, after DNA-MB-MWNTs/GCE had interacted with 1.0 mM QN or QD enantiomers for 10 min, the anodic peak currents were decreased, suggested the interaction between the modified electrodes and enantiomers had been introduced a barrier on the electrode surface for electron transfer. A larger decrease was obtained from QD, in which I_{QN} was 68.94 μA (Scheme.1b) while I_{QD} was 51.60 μA (Scheme.1c). The current difference ($\Delta I = I_{QN} - I_{QD}$) got to 17.34 μA, with relative standard deviations (*RSD*) of 2.4% (n = 7), resulted from the enantioselective interaction of DNA with QN and QD. So, the proposed sensing platform could be not only used as mediator to shuttle electrons between analyte and electrode surface but also acted as chiral probe for QN and QD.

To explore the role of DNA, contrast experiments were done by MB-MWNTs/GCE under the same conditions (Fig.7A). Almost the same decrease in peak currents were observed for QN and QD (n = 7, *RSD* = 1.2%), implying drug stereoisomers could not be discriminated in the absence of DNA. DNA, acted as a chiral selector, has an important indispensable factor to achieve the enantioselective recognition.

In addition, as another comparative experiment, DNA/MB-MWNTs/GCE were also used to interact with 1.0 mM QN or QD under the same conditions (Fig.7B). Current difference about 6.0 μA was observed from QD and QN (n = 7, *RSD* = 4.5%). It was obviously that both DNA-MB-MWNTs/GCE (the inset of Scheme 1) and DNA/MB-MWNTs/GCE (Fig.7B) exhibited stronger affinity to QD, while the current difference of the developed sensing platform was about 3 times higher than that of the comparative one. This might attribute to the application of biomolecule-based nanocomposite, combining the stereoselective properties of DNA with the signal amplification feature of nanomaterial. The performance of chiral sensor depends on the nature of chiral selector and the effective immobilization of these molecules. The application of nanomaterial could provide a superior microenvironment for biological molecules to enhance the enantioselective interaction in chiral analysis.[32]

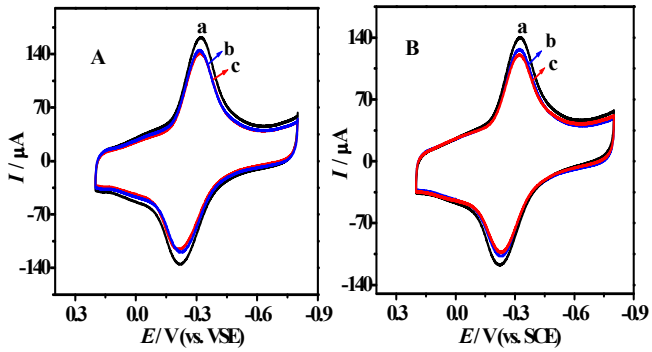

Fig.7 The CVs of (A) (a) MB-MWNTs/GCE and (B) (a) DNA/MB-MWNTs/GCE and the two modified electrodes had interacted with 1.0 mM (b) QN and (c) QD for 10 min, respectively. Other conditions, as in Scheme 1

DNA, containing rich functional active groups such as amino groups and carbonyl groups, could bind with drug molecules through electrostatic interactions, hydrogen bond and hydrophobic interactions.[33,34] QN and QD, as shown in Fig.1, can provide several binding sites for molecular interaction, such as the basic nitrogen group of the quinuclidine ring for electrostatic interaction, the carbamate group for hydrogen bonding and dipole - dipole interaction, the π - basic quinoline ring for intermolecular π - π interaction, the bulky quinuclidine group and the large planar quinoline ring for steric interaction.[20] Quinine/quinidine pairs that possess opposite configurations at the relevant stereogenic centers (C8 and C9), exhibited a crucial role in effective chiral recognition.[35] There is no consensus yet about the interaction between cinchona derivatives and DNA. Some

researcher tended that QN could interact with DNA to form complexes by hydrogen bond.[36] While other thought that QN had intercalated into DNA, in which alkaloids molecules, with the lipophilic and planar of a size, fitted well between the GC and AT stacks of the DNA double helix.[37] No matter which kind of force they are, the interaction both QN and QD to the chiral sensing platform could introduce a barrier to electron transfer, resulting in a decrease in the peak current signals. The spatial arrangements of QN may match better with the chiral selector (DNA), so larger amount of QD was adsorbed on the electrode surface, resulting in a bigger hindrance in electrochemical response (as illustrated in Scheme.1).

3.4 Optimization of the sensing conditions

The acidity of the prepared solution could greatly affect the surface charge properties of chiral drugs. By taking into account the p*K*a value of the QN and QD (4.2 and 8.8), DNA-MB-MWNTs/GCE was used to examine the solutions of 1.0 mM QN or QD prepared in 0.1 M PBS from pH 2.0 to pH 6.0. Table 1 summarized the effect of pH on the enantioselectivity coefficient (α). The observed results supported that the electrochemical difference for QN and QD mainly originated from its protonated species, and the best selectivity (α = 2.47) was achieved at pH 4.0. So, PBS in pH 4.0 was used to prepared the QN and QD solution to study enantioselective interaction. The selectivity coefficient (α) was calculated from formula (1):[38]

$$\alpha = \frac{\Delta I_{QD}}{\Delta I_{QN}} \qquad (1)$$

Where α is the enantioselectivity coefficient, a quantitative measure of a sensor's ability to discriminate enantiomers, ΔI_{QD} and ΔI_{QN} are the averaged difference of the anodic peak currents after the proposed electrodes correspond to QN and QD (n = 7).

Table 1 Effect of the solution pH on the enantioselectivity coefficient (α).

pH	ΔI_{QN} (μA)	ΔI_{QD} (μA)	α
2.0	10.02	14.54	1.45
2.5	11.41	17.97	1.57
3.0	11.69	20.36	1.74
3.5	12.77	25.52	2.00
4.0	13.7	31.04	2.27
4.5	13.59	27.19	2.00
5.0	9.34	18.7	2.00
5.5	8.76	17.22	1.97
6.0	6.78	11.97	1.77

The difference of peak current (ΔI_{QN} or ΔI_{QD}) at different interaction time was exhibited in Fig.8. After DNA-MB-MWNTs/GCE incubated in 1.0 mM QN or QD, both the ΔI_{QD} and ΔI_{QN} increased continuously with the reaction time, but ΔI_{QD} was always larger than ΔI_{QN} at the same time. When the time was up to 10 min, no larger difference between ΔI_{QD} and ΔI_{QN} was observed with the prolongation of incubation time. So, 10 min was chosen as the optimal reaction time.

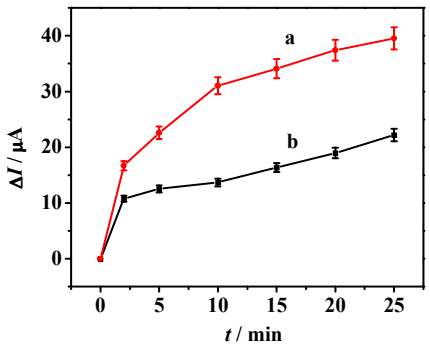

Fig.8 The relationship between peak current difference (ΔI) and incubation time after DNA-MB-MWNTs/GCE in 1.0 mM (a) QD and (b) QN. Other conditions, as in Scheme 1.

3.5 Validation of the proposed sensor

To evaluate the repeatability of the preparation procedure, seven modified electrodes with the same fabrication process (DNA-MB-MWNTs/GCE) were used to detect the electrochemical response in 0.1 M PBS buffer solution. The seven measurements had presented no significant difference among the peak currents, with *RSD* of 2.5%. In addition, 98.3% of the initial peak current was observed after 20 cycles successive measurements on a single electrode (n = 7, *RSD* = 2.4%), indicating the sufficient stability of the prepared nanocomposite on the surface of GCE.

The precision of the proposed sensor was monitored by performing seven replicate measurements in detecting 1.0 mM QN and QD, respectively. Peak current of 68.94 ± 1.4 μA for QN and 51.60 ± 0.9 μA for QD were achieved (intra-assay, n = 7), and that of 67.60 ± 1.9 μA for QN and 51.12 ± 1.6 μA for QD were obtained over five days (inter-assay, n = 7). The results indicated acceptable repeatability and reproducibility of the sensing platform for enantioselective interaction with QN and QD. The long-term storage stability of the sensing platform was examined after the proposed electrodes had stored at 4°C for 15 days. The peak current retained about 97.6% (QN) or 98.2% (QD) of its initial response, suggesting an excellent stability of the sensing platform (n = 7).

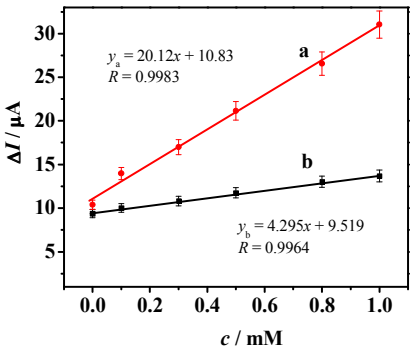

Fig.9 Current decreasing of DNA-MB-MWNTs/GCE with various concentrations of (a) QD and (b) QN for 10 min: 0.1 mM, 0.3 mM, 0.5 mM, 0.8 mM, 1.0 mM. Other conditions as in Scheme 1.

To evaluate the enantioselective response, analysis of QN or QD solutions at six concentrations was studied on variation of the current difference by seven replicate measurements under the optimized conditions (Fig.9). It could be seen that ΔI_{QD} kept

larger than ΔI_{QN} due to the specific interaction between DNA and QD. In addition, ΔI_{QD} and ΔI_{QN} increased linearly with the rising concentration of QN and QD over the range 0.1 mM to 1.0 mM. The results further confirmed that the developed sensor had a higher stereoselective affinity to QD.

3.7 Application of enantioselective sensor

Under the optimal experimental conditions, the chiral sensing platform was used to measure the mixtures of QN and QD. The detection solutions were prepared by changing the proportion of QD from 0 to 100% with the total concentration being kept at 0.1 mM and 1.0 mM. Seven parallel modified electrodes have been used to determine the value for every proportion of QD, and the variation currents were presented in Table *S*1 (Supporting Information). Meanwhile, five replicate experiments were conducted to ensure the reliability of the proposed method, and the inter-assay *RSD* were obtained below 3.0%, resulting from the good precision and reproducibility of the sensing platform. As shown in Fig.10, the peak current was gradually decreased along with the rising ratio of QD, due to the higher affinity for proposed platform and QD. The enantiomeric ratio of QD was proportional to the current response, and the calibration plots were expressed by the liner regression equations as $I_{0.1\ mM}$ = -0.1806 *QD%* + 70.32 (R^2 = 0.9780) and $I_{1.0\ mM}$ = -0.1518 *QD%* + 73.20 (R^2 = 0.9926), respectively.

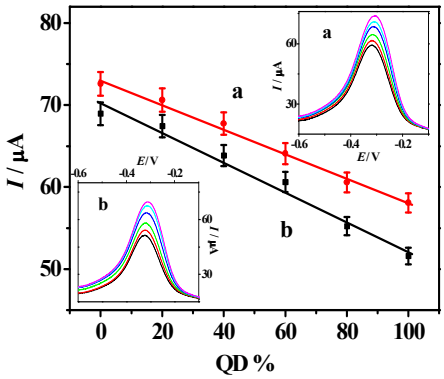

Fig.10 Current response of enantiomeric composition of QN and QD at different concentrations: (a) 1.0 mM; (b) 0.1 mM. Insets: the peak currents with different concentrations. Other conditions as in Scheme 1.

Conclusions

In this article, a novel biomolecule-based nanocomposite, cooperating the stereoselective properties of DNA and signal amplification feature of functionated nanomaterial, was prepared to fabricate the chiral sensing platform for enantioselective recognition of QN and QD. The comparative performance between the proposed strategy and the traditional method (prepared by adsorbing MB-MWNTs on GCE for further binding of DNA), were investigated. The results demonstrated the proposed sensing platform could not only simplify the assemble process, but also enhance the chiral discrimination of QN and QD. Such design, with the advantage of simple preparation, good stability and excellent reproducibility, may provide a reference for the development of electrochemical chiral sensor.

Acknowledgment

The authors are grateful for the financial supports provided by the National Natural Science Foundation of China (21272188).

Notes and references

Laboratory of Luminescence and Real-Time Analysis (Southwest University), Ministry of Education, College of Chemistry and Chemical Engineering, Southwest University, Chongqing 400715, China. Corresponding author: Fax: +86-023-68253195; Tel: +86-023-68252360; E-mail address: fyzc@swu.edu.cn

1 G. Q. Lin, J. G. Zhang and J. F. Cheng, *Chiral Drugs: Chemistry and Biological Action*, ed. G. Q. Lin, Q. D. You and J. F. Cheng, 2011, vol. 1, ch. 1, pp. 1-27.
2 A. Cavazzini, L. Pasti, A. Massi, N. Marchetti and F. Dondi, *Anal. Chim. Acta*, 2011, **706**, 205.
3 J. Haginaka, *J. Chromatogr. A.*, 2000, **875**, 235.
4 J. W. Chen, Y. S. Hsieh, J. Cook, R. Morrison and W. A. Korfmacher, *Anal. Chem.*, 2006, **78**, 1212.
5 S. S. Yu, W. Plunkett, M. Kim and L. Pu, *J. Am. Chem. Soc.*, 2012, **134**, 20282.
6 W. C. Su, W. G. Zhang, S. Zhang, J. Fan, X. Yin, M. L. Luo and S. C. Ng, *Biosens. Bioelectron.*, 2009, **25**, 488.
7 Y. Z. Fu, Q. Chen, J. Zhou, Q. Han and Y. H. Wang, *Anal. Biochem.*, 2012, **421**, 103.
8 R. I. Stefan, J. K. F. van Staden and H. Y. Aboul-Enein, *Electroanalysis*, 1999, **11**, 1233.
9 J. J. Gooding, *Electrochim. Acta,* 2005, **50**, 3049.
10 G. M. do Nascimento, R. C. de Oliveira, N. A. Pradie, P. R. G. Lins, P. R. Worfel, G. R. Martinez, P. D. Mascio and M. S. Dresselhaus, P. Corio, *J. Photochem. Photobiol. A.*, 2010, **211**, 99.
11 M. C. Kum, K. A. Joshi, W. Chen, N. V. Myung and A. Mulchandani, *Talanta*, 2007, **74**, 370.
12 G. M. Do Nascimento, P. Corio, R. W. Novickis, M. L. A. Temperini and M. S. Dressel-haus, *J. Polym. Sci. Part A: Polym. Chem.*, 2005, **43**, 815.
13 B. Xue, P. Chen, Q. Hong, J. Y. Lin and K. L. Tan, *J. Mater. Chem.*, 2001, **11**, 2378.
14 X. W. Wei, X. J. Song, J. Xu, Y. H. Ni and P. Zhang, *Mater. Chem. Phys.*, 2005, **92**, 159.
15 S. Pakapongpan, R. Palangsuntikul and W. Surareungchai, *Electrochimi. Acta*, 2011, **56**, 6831.
16 M. Guo, J. H. Chen, D. Y. Liu, L. H. Nie and S. Z. Yao, *Bioelectrochemistry*, 2004, **62**, 29.
17 Y. Matsuoka, N. Kanda, Y. M. Lee and A. Higuchi, *J. Membr. Sci.*, 2006, **280**, 116.
18 L. Zhang, M. F. Song, Q. Tian and S. G. Min, *Sep. Purif. Technol.*, 2007, **55**, 388.
19 Y. H. Wang, Q. Han, Q. Zhang, Y. H. Huang, L. J. Guo and Y. Z. Fu, *J Solid State Electrochem.*, 2013, **17**, 627.
20 M. Lammerhofer and W. Lindner, *J. Chromatogra. A.*, 1996, **741**,33.
21 K. Schug, P. Fryčák, N.M. Maier and W. Lindner, *Anal. Chem.*, 2005, **77**, 3660.
22 S. Zaugg and W. Thormann, *J. Pharm. Biomed. Anal.*, 2001, **24**, 785.
23 J. Caldwell, J. Chromatogr. A, 1996, **719**, 3.
24 M. Lanz, R. Theurillat, W. Thormann, *Electrophoresis*, 1997, **18**. 1875.
25 Q. Zhou, M. A. McCracken and J. S. Strobl, *Breast cancer Res Tr.*, 2002, **75**, 107.

26 L. Y. Zhao, H. Y. Liu and N. F. Hu, *Anal Bioanal Chem*, 2006, **384**, 414.

27 T. Sagara, H. Kawamura and N. Nakashima, *Langmuir,* 1996, **12**, 4253.

28 Y. Y. Shao, J. Wang, H. Wu,J. Liu,I. A. Aksay ,Y. H. Lin, *Electroanalysis*, 2010, **22**, 1027.

29 H. G. Wei, H. B. Gu, J. Guo, S. Y. Wei and Z. H. Guo, *J. Electrochem. Soc.*, 2013, **160**, G3038.

30 W. Sun, X. Z Wang, Y. H. Wang, X. M. Ju, L. Xu, G. J. Li and Z. F. Sun, *Electrochim. Acta*, 2013, **87**, 317.

31 S. B. Khoo and F. Chen, *Anal. Chem.*, 2002, **74**, 5734.

32 D. Chen, G. Wang, J.H. Li, *J. Phys. Ch*em. C., 2007, **111**, 2351.

33 L. L. Shen, L. A. Mitscher, P. N. Sharma, T. J. O'Donnel1, D. W. T. Chu, C. S. Cooper, T. Rosen and A. G. Pernet, *Biochemistry*, 1989, **28**, 3886.

34 M. L. Kopka, C. Yoon, D. Goodsell, P. Pjura and R. E. Dickerson, *Proc. Natl. Acad. Sci*, 1985, **82**, 1376.

35 C. Czerwenka, M. La1mmerhofer, N. M. Maier, K. Rissanen, W. Lindner, *Anal. Chem.*, 2002, **74**, 5658.

36 R. L. O'Brien, J. G. Olenick and F. E. Hahn, *Proc. Natl. Acad. Sci.*, 1966, **55**, 1511.

37 M, Wink, T, Schmeller, B. Latz-bruning, *J. Chem. Ecol*, 1998, **24**, 1881.

38 Y. X Wang, X. L Yin, M. H Shi, W. Li, L. Zhang and J. L. Kong, *Talanta*, 2006, **69**, 1240.

A table of contents entry

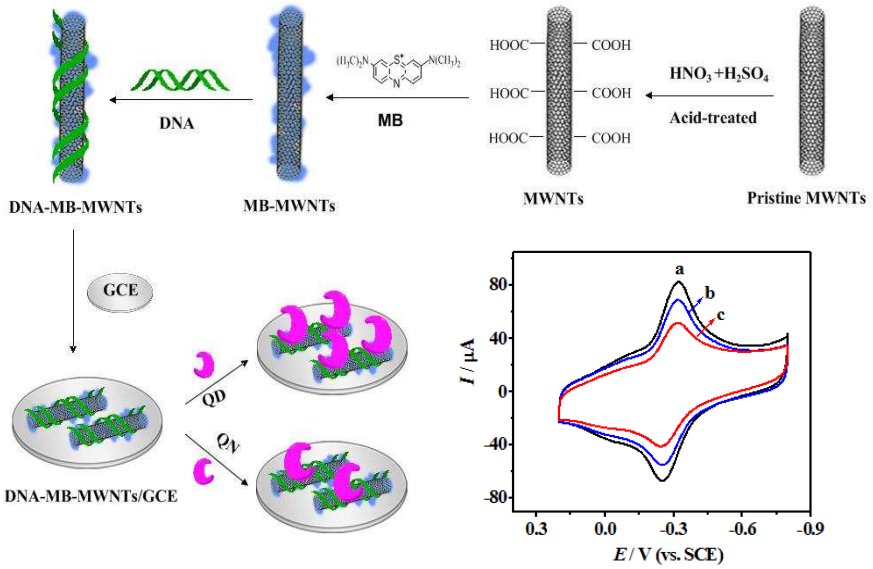

The DNA-based nanocomposite was prepared to develop a simple strategy for electrochemical chiral analysis.